Available online at www.sciencedirect.com
SCIENCE DIRECT®
International Journal of Heat and Mass Transfer 47 (2004) 4881–4893
International Journal of HEAT and MASS TRANSFER
www.elsevier.com/locate/ijhmt

Frost formation on a plate with different surface hydrophilicity

Hyunuk Lee [a,1], Jongmin Shin [a,*], Samchul Ha [a,2], Bongjun Choi [a,1], Jaekeun Lee [b,3]

[a] *Digital Appliance Co. Research Laboratory, AC & R Team, LG Electronics Inc., 391-2 Gaeumjeong-Dong, Changwon, Kyoungnam 641-711, South Korea*

[b] *30 Jangjeon-Dong, Geumjeong-Gu, Pusan 609-735, South Korea*

Received 13 June 2003; received in revised form 11 March 2004
Available online 21 July 2004

Abstract

The objectives of this study are to develop frost maps for two different surfaces having two different hydrophilic characteristics and to find ambient conditions associated with the formation of frost structures. Test samples with two different surfaces having dynamic contact angle (DCA) of 23° and 88° were installed in a wind tunnel and exposed to a humid airflow. Frost structure is observed with a visualization system in the operating conditions of household refrigerator: airflow temperature in the range of +10–20 °C, humidity in the range of 2.64–9.36 g/kg′, Reynolds number in the range of 7000–17,000 and cold plate temperature in the range of −11.6 to −28.4 °C. As results of this study, frost structures are classified and frost maps are proposed for two different surface hydrophilicities. Surface with low DCA (23°) shows lower frost thickness and higher frost density than that with high DCA (88°). It was found that frost structures on surfaces with different DCA are similar. However, low DCA surface at low humidity provides 20–30% denser frost formation due to the shift of areas with different structures.

Keywords: Fin-and-tube heat exchanger; Surface characteristics; Frost; Hydrophilic; Hydrophobic; Dynamic contact angle

1. Introduction

Frost is a well-known phenomenon occurring on a cold surface when water vapor in the surrounding air adheres to the cold surface through heat and mass transfer. Frost layer on the cold surfaces of the heat exchanger adversely affects the performance of the refrigerating unit due to the increase of the air pressure drop and the decrease of thermal efficiency. Defrost process is required to remove frost layer on the cold surfaces in most applications and electric heaters accompanied with energy and time are applied to melt those frost layer periodically. Practically, there are no clear and reliable methods to prevent frost formation on cold surfaces of refrigeration system. Thus, designers of refrigeration system should account the negative contribution of frost in their work in order to provide normal performance even when the devices are completely covered by frost. Many scientific researches have been focused on the investigation of frost structure to manage frost layer efficiently in the applications of refrigeration systems.

Hayashi et al. [1] proposed the frost map and growth model with four types of crystals. They described the characteristics of each frost structure in detail and studied frost properties. However, boundaries between different region are unclear and cold plate temperature range in their map has limitation of

* Corresponding author. Tel.: +82-55-260-3828; fax: +82-55-260-3507.
E-mail addresses: hyunuk@lge.com (H. Lee), shinjm@lge.com (J. Shin), samha@lge.com (S. Ha), choibj@lge.com (B. Choi), jklee@pusan.ac.kr (J. Lee).
[1] Tel.: +82-55-260-3828; fax: +82-55-260-3507.
[2] Tel.: +82-55-260-3820; fax: +82-55-260-3507.
[3] Tel.: +82-51-510-2455; fax: +82-51-512-5236.

0017-9310/$ - see front matter © 2004 Elsevier Ltd. All rights reserved.
doi:10.1016/j.ijheatmasstransfer.2004.05.021

Nomenclature

A	cross-section area test sample, m^2
A_c	flow cross-section area, m^2
ADCA	advanced dynamic contact angle, deg
DCA	dynamic contact angle, deg
D_h	hydraulic diameter, m
F	force, N
g	gravity, m/s^2
L	depth immersed in water, m
m	frost mass, g/m^2
p	wetted perimeter of test sample
P_c	wetted perimeter of air flow channel
Re	Reynolds number
T_p	plate temperature, °C
V	velocity, m/s
W	absolute air humidity, g/kg′

Greek symbols

δ	frost thickness, mm
θ_D	dynamic contact angle, deg
ρ	frost density, kg/m^3
ρ_l	density of liquid, kg/m^3
ρ_v	density of vapor (air), kr/m^3
σ	surface tension, dyne/m
v	kinematic viscosity, m^2/s

Subscripts

c	cross-sectional of air flow
h	hydrodynamic
l	liquid
p	plate
v	vapor

−20 °C and airflow velocity is too high for commercial refrigerating system. Simplified approach with the frost map with two types of frost crystals was described by Tokura et al. [2] for free convection conditions. Authors analyzed the crystal shape and predicted the formation of thicker frost layer with lower density for more intensive mass transfer conditions. Sahin [3] analyzed literature data on frost crystal formation at various temperatures of the surface and found physical background for the formation of needle-type and plate-type crystals at frost. Author described in his study that frost shape strongly depends on plate surface temperature. Ohkubo [4] investigated frost formation on supercooled surfaces for forced convection condition and proposed the frost map with needle-type and dendrite-type crystals.

It is well known that frost formation depends strongly on air velocity, air humidity, air temperature and cold surface temperature. Thus numerous researchers had studied influence of ambient conditions and wall temperature on frost growth. Moreover, current frost management schemes for refrigeration systems usually rely on achieving frost tolerance through geometric design. Approach of Hmaladze and Chepurnenko [5] was based on the studies of frost structures formed on finned surfaces with different shape of fins. Ogawa et al. [6] studied design optimization to provide more uniform frost formation and less pressure drop. Meanwhile, few works had been performed to investigate the effect of surface hydrophilicity on frost formation and reported results were contradicted. It is believed that one of more advanced and attractive methods is the surface hydrophilicity of the plate because that of the fin surfaces has a profound effect on the nature of the frost growing. Nikulshina et al. [7] studied the application of hydrophobic organic coating to change frost structure. Seki et al. [8] and Hoke et al. [9] investigated the frost structure for hydrophobic coating. The authors reported that denser frost layer was formed on a lower surface energy, i.e., on hydrophobic surface rather than hydrophilic one. Ryu and Lee [10] studied frost formation in fin-and-tube heat exchanger with different surface energies and came to contrary conclusion. They found that frost thickness for hydrophilic heat exchanger became thinner with smaller airside pressure drop, than that of conventional aluminum heat exchanger. Shin et al. [11] found that hydrophilic surfaces having lower dynamic contact angle provides the denser frost on the plate at the test condition of home refrigerators. Thus, detailed analysis on the frost formation with respect to different surface hydrophilicity will provide design guideline for heat exchanger of refrigerating system.

Objectives of the present study on frost phenomenon are: (1) to develop the frost map for operating conditions of home refrigerators with regards to hydrophilic and hydrophobic surface, and (2) to find ambient conditions providing formation of denser frost.

2. Test program

2.1. Test samples

Two types of plates with known dynamic contact angle (DCA) were tested: aluminum plates having DCA of 88° and the hydrophilic coating plates having DCA of 23°. The hydrophilic plates were obtained by means of a new technology of plasma polymerization described by Kim et al. [12].

2.2. Measurement of surface hydrophilicity

The dynamic contact angle that represents surface hydrophilicity of the plate was measured using Wilhemy plate method as shown in Fig. 1(a). During measurements test samples were moved into water with constant velocity downward to the gravity direction. The tangential angle of the water to the surface made during this period is called the advanced DCA. All forces acting on the sample, such as the gravity, buoyancy of the sample, surface tension and the force of sustain the sample should be in equilibrium as shown in Fig. 1(b) can be expressed by Eq. (1).

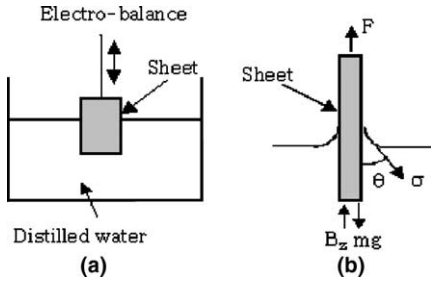

Fig. 1. Measuring method for surface hydrophilicity: (a) schematic diagram and (b) equilibrium forces.

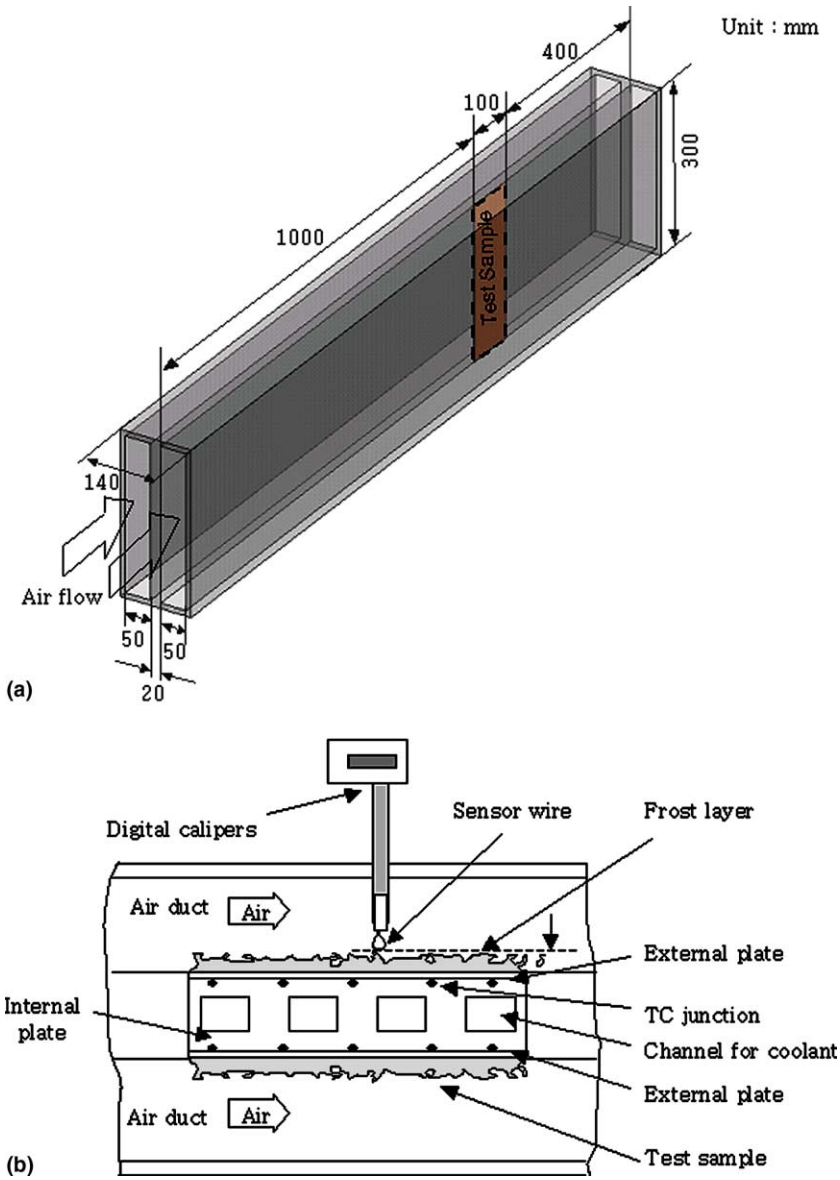

Fig. 2. Design of test sample with location of thermocouples and design of the sensor for frost thickness acquisition.

$$F = p\sigma\cos\theta_D - (\rho_l - \rho_v)gAL \quad (1)$$

where, F is the force measured by the electro-balance (SIGMA 70: model KSV, 77000B), p is the wetted perimeter of sheet, σ is the surface tension of distilled water, A is the cross-section area of test sample immersed in liquid, L is the depth immersed in water, g is the gravity force, ρ is the density, and θ_D is the DCA. The term $(\rho_l - \rho_v)gAL$ is the buoyancy force. The DCA is given by

$$\cos\theta_D = \frac{F/L - (\rho_v - \rho_l)gA}{p\sigma/L} \quad (2)$$

Details of contact angle measurement process and uncertainty of measurements are well described in Shin et al. [13].

2.3. Design of test section

Fig. 2 shows the design of test section with the locations of thermocouples and sensors for frost thickness acquisition. Test samples were embraced by thick plates made of aluminum alloy and had the size of 100 mm length in the airflow direction, and those widths

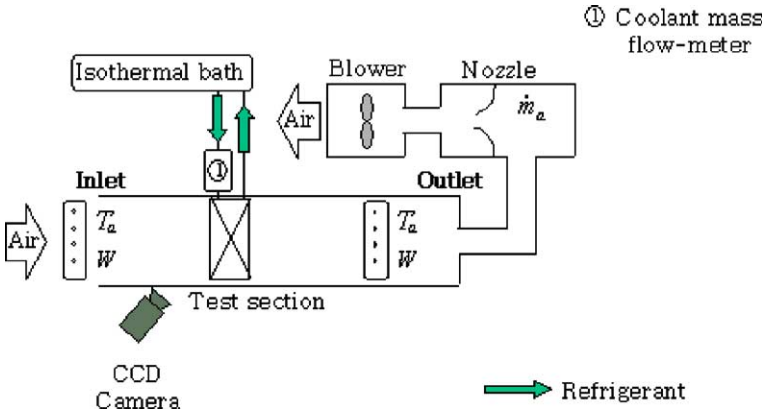

Fig. 3. Experimental apparatus for frosting tests (tests were conducted in a psychrometric chamber).

Table 1
Test conditions and results after 30 min of frost deposition on hydrophobic surface

Test number	Conditions			Results of frost measurements		
	W (g/kg′)	T_p (K)	Re	δ (mm)	M (kg/m^2)	ρ (kg/m^3)
1	2.64	253.15	12,000	0.72	0.0732	101.6
2	4	248.15	9000	1.37	0.0918	67
3	4	253.15	15,000	1.42	0.1162	81.8
4	4	258.15	9000	0.84	0.0864	102.8
5	4	258.15	15,000	1.13	0.1157	102.4
6	4	263.15	9000	0.36	0.0667	185.2
7	5.5	253.15	9000	2.27	0.1217	53.6
8	5.5	263.15	15,000	1.16	0.1357	117
9	6	244.75	12,000	2.25	0.1559	69.3
10	6	253.15	6955	2.09	0.1127	53.9
11	6	253.15	12,000	2.12	0.159	75
12	6	253.15	12,000	2.07	0.1565	75.6
13	6	253.15	12,000	2.18	0.1589	72.9
14	6	253.15	12,000	2.13	0.154	72.3
15	6	253.15	12,000	2.12	0.1579	74.5
16	6	253.15	12,000	2.12	0.156	73.6
17	6	253.15	17,045	2.23	0.1982	88.9
18	6	261.55	12,000	1.51	0.154	102
19	8	248.15	9000	2.26	0.1808	80
20	8	248.15	15,000	2.28	0.2472	108.4
21	8	258.15	9000	1.81	0.17	93.9
22	8	258.15	15,000	1.86	0.2355	126.6
23	9.36	253.15	12,000	2.25	0.2549	113.3

were 300 mm. Four rectangular channels with cross-sectional area of 10×10 mm^2 inside internal thick plate were consisted to provide coolant flow. Also 10 grooves were engraved on both internal plates to install the 0.127 mm diameter T-type thermocouples (TT-T-36, OMEGA). After installation, thermocouples were covered by thermal paste (D-500, DOTITE) with thermal conductivity of 30 W/(m K). Then two thin external plates made of aluminum alloy were attached to the internal thick plates. Five thermocouples on each side were installed to acquire the averaged cold plate temperature. For calculation of heat flux, coolant temperatures at inlet and outlet were controlled by RTD (100 Ω, CHINO). Four fine thermocouples (COCO-001, OMEGA) with 25 μm diameter electrodes were used for acquisition of temperature profile along the frost layer. To obtain frost thickness, peculiar sensing method was applied with digital calipers and 25 μm diameter wire sensor as shown in Fig. 2. Maximum detected value through the digital calipers when the sensor wire touched to the top of the frost layer assumed to be the frost layer thickness. Movement and measurement by touching method were controlled by visualization system.

2.4. Frosting test

The schematic diagram of experimental apparatus is shown in Fig. 3. It consists of three independent parts: a psychrometric chamber, a coolant supply loop and a wind tunnel test facility. The psychrometric chamber included an air-handling unit with compressors, a 10 kW humidifier and 7 kW heaters and air-sampling unit. Three compressors with the capacity of 1.5, 2.5, and 4.0 kW were available, and appropriate ones could be selected to provide the desirable temperature in the range of +5–+20 °C and relative humidity (RH) from 40% to 80%, which correspond to absolute humidity in the range of 2.64–9.36 g/kg′. Airflow humidity is controlled both at the entrance of the wind tunnel and after the test section. For this purpose, dry and wet air temperature were measured by platinum resistance temperature sensor, RTD (100 Ω, CHINO), with the accuracy of ±0.05 °C. Airflow velocities, Reynolds number from 6955 to 17,045 in the present study, were obtained according to ASHRAE standard [14] employing nozzle and pressure drop measurement along it. Reynolds number is defined as follows.

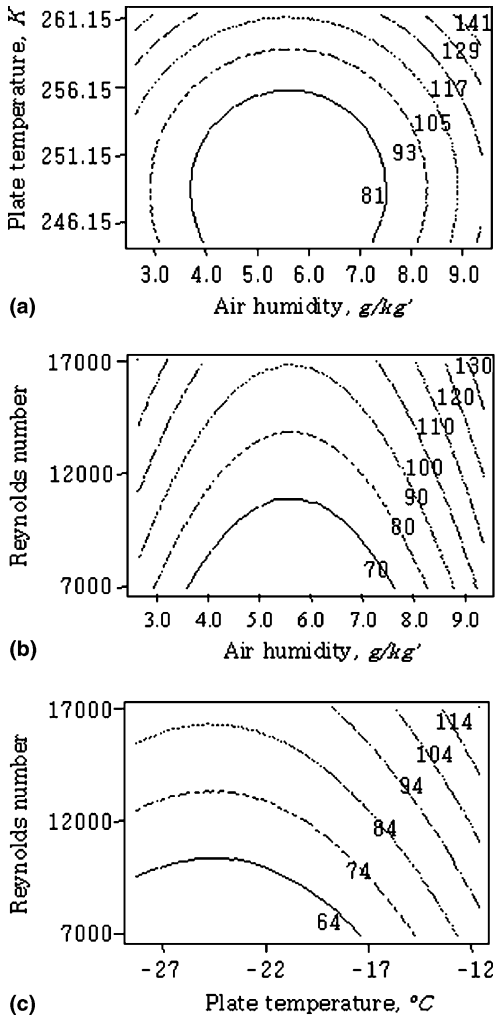

Fig. 4. Contour plots of frost density as the functions of operating parameters after 30 min of frost deposition on hydrophobic surface: (a) $Re = 12{,}000$, (b) $T_p = -20$ °C, and (c) $W = 6.0$ g/kg′.

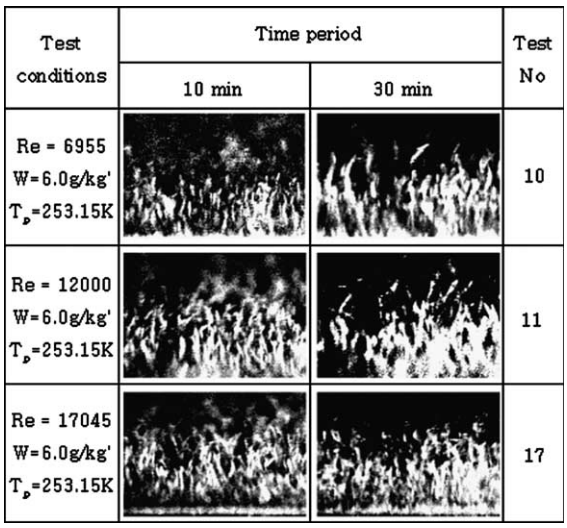

Fig. 5. Frost images for different Reynolds number after 10 and 30 min on hydrophobic surface.

$$Re = \frac{VD_h}{v} \tag{3}$$

where, V is the velocity, D_h is the hydraulic diameter and v is the kinematic viscosity. The hydraulic diameter is defined as

$$D_h = \frac{4A_c}{P_c} \tag{4}$$

where, A_c and P_c are the flow cross-sectional area and the wetted perimeter of air flow channel, respectively.

The test section was made of transparent acrylic material with thickness and length of 10 and 1500 mm, respectively. Airflow passes through the mesh for smoothening and the cross-section area of 120 mm × 300 mm, which was divided in the middle by 20 mm thick acrylic plate. Frost deposited on the both sides of the sample. The coolant supply loop contained a stainless steel bath with heaters and heat exchanger connected to a low-temperature refrigerating unit. Such a design provided maintenance of constant coolant temperature in the range from −30 to −5 °C with the accuracy of ±0.2 °C. A stainless steel pump and a mass flow meter were used to obtain constant coolant flow rate. The coolant was the mixture of water and ethylene glycol by 50 to 50 percent in weight. To obtain images for frost growing, visualization system consisted of CCD camera (VX-1,

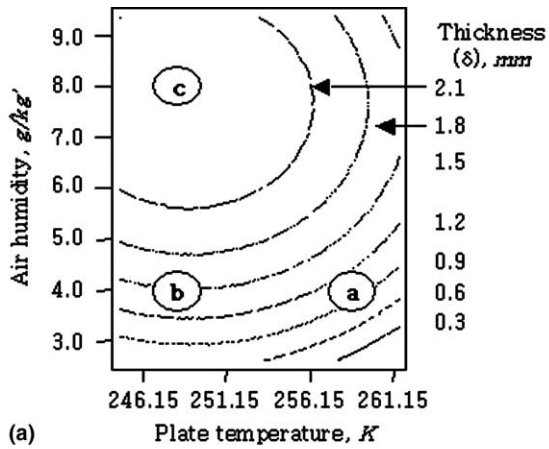

Point	Test conditions	Time period		Test No
		10 min	30 min	
a	Re = 9000 W=4.0g/kg' T_p=258.15K	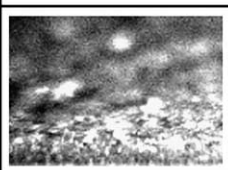	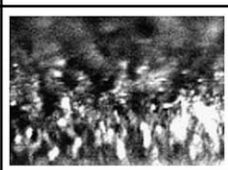	4
b	Re = 9000 W=4.0g/kg' T_p=248.15K	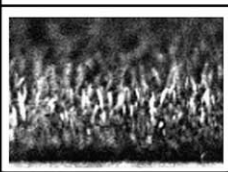	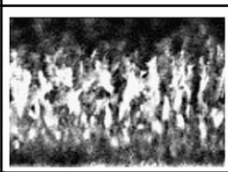	2
c	Re = 9000 W=8.0g/kg' T_p=248.15K	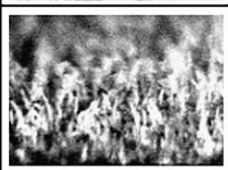	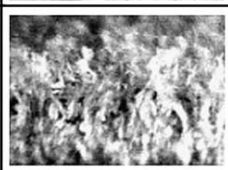	19

(b)

Fig. 6. Frost structures and thickness profile for different air humidity and plate temperatures at Reynolds number of 9000 on hydrophobic surface: (a) contour plot and (b) frost images.

SONY) with 25 times magnifying lens and computer was employed shown in Fig. 3. Images of frost structure were recorded after 5, 10, 20 and 30 min. Simultaneously, the weight of the sample with deposited frost was obtained by weighing machine with precision scale (TP-2KS, OHAUS). Then it was dried by fan and weighed again to calculate pure frost mass deposited. The accuracy of the measurement was ±0.00001 kg.

3. Test results

3.1. Frost map for hydrophobic surface

Test sample having the DCA of 88°, uncoated bare aluminum surface, was used to develop frost map for hydrophobic surface. Test conditions are chosen by the design of experiment (DOE) as combination of airflow

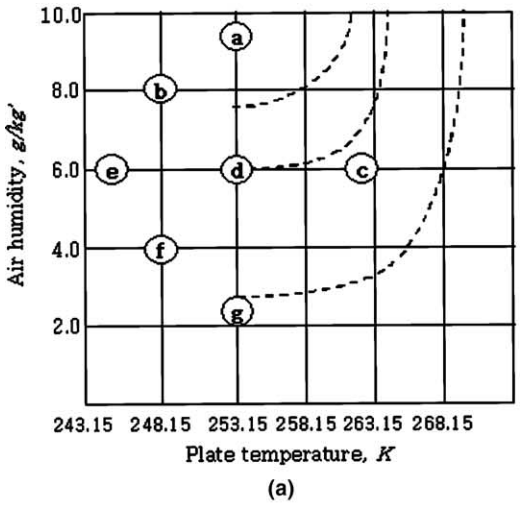

(a)

Type of crystal structure	Point	Test conditions	Image of crystal structure	Test No
Feather-type crystal structure	a	Re =12000 W= 9.36g/kg' T_p=253.15K		23
	b	Re = 9000 W= 8.0g/kg' T_p=248.15K		19
Grass-type crystal structure	c	Re =12000 W= 6.0g/kg' T_p=261.55K		18
	d	Re =12000 W= 6.0g/kg' T_p=253.15K		11
	e	Re =12000 W= 6.0g/kg' T_p=244.75K		9
	f	Re = 9000 W= 4.0g/kg' T_p=248.15K		2
Plate-type crystal structure	g	Re =12000 W= 2.64g/kg' T_p=253.15K		1

(b)

Fig. 7. Frost map with the test conditions and frost images generated on hydrophobic surface after 30 min: (a) comparison with frost map by Hayashi, (b) frost images --- frost map by Hayashi et al. [1], ○ locations of test condition in present study.

humidity, cold plate temperature, and Reynolds number and similar to those in home refrigerators; airflow humidity in the range of 2.64–9.36 g/kg′, airflow temperature in the range of +10–20 °C, Reynolds number in the range of 7000–17,000 and cold plate temperature in the range of −11.6 to −28.4 °C. Table 1 shows the test conditions and the results of frost measurements including frost thickness, mass and density. From test results as shown in Table 1, analysis are as follows:

1. Frost thickness increases with the increase of airflow humidity and the decrease of cold plate temperature, but it is slightly affected by air Reynolds number. Similar conclusion were made in Hayashi et al. [1] and Lee et al. [15].
2. Frost density increases with the decrease of the air humidity. Frost layer is denser with the increase of cold plate temperature. Similar trends were observed in the study of Mao et al. [16].
3. Deposited frost mass increases with the increase of airflow humidity and decrease of cold plate temperature. Ostin and Anderson [17] founded the same trends for frost mass accumulation.
4. Higher airflow humidity causes on more massive, thicker and less dense frost, as reported by Mao et al. [16]. This phenomenon may be explained as the increase of mass transfer due to larger humidity differences and the deposition of large frost mass.

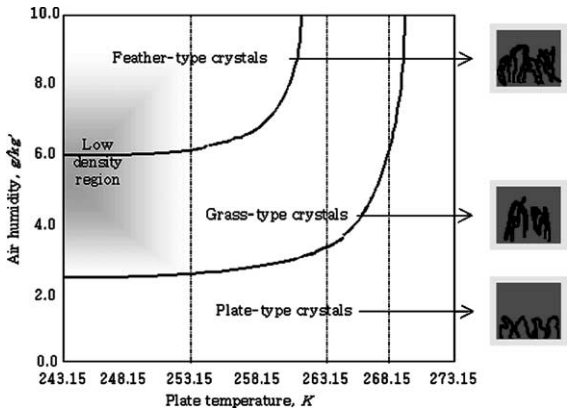

Fig. 8. Proposed frost map for hydrophobic surface.

Fig. 4 shows the contour plots for frost density as function of airflow humidity, Reynolds number and plate surface temperature. Values of the density were obtained after 30 min of continuous frost deposition. When cold plate temperature drops to −20 to −27 °C and humidity is within 4.0–7.0 g/kg′, grass-type crystals prevail in frost formation and those become more porous as time being at the test conditions. Frost density is small for all Reynolds number inside this region. Especially when Reynolds number is 6955, frost density drops even below 60 kg/m^3. Such a phenomenon may be classified by specific growth mode of frost crystals. The

Table 2
Test conditions and results after 30 min of frost deposition on hydrophilic surface

Test number	Conditions			Results of frost measurements			
	W (g/kg′)	T_p (K)	Re	From present study			Table 1
				δ (mm)	m (g/m^2)	ρ (kg/m^3)	ρ (kg/m^3)
1	2.64	253.15	12,000	0.52	0.0688	132.4	101.6
2	4	248.15	9000	1.33	0.0891	67	67
3	4	248.15	15,000	1.32	0.1185	89.8	86
4	4	258.15	9000	0.73	0.0898	123	102.8
5	4	258.15	15,000	1.05	0.1143	108.9	102.4
6	6	244.75	12,000	2.45	0.1553	63.4	69.3
7	6	253.15	6955	1.91	0.1066	55.8	53.9
8	6	253.15	12,000	2.18	0.1576	72.3	75
9	6	253.15	12,000	2.21	0.1602	72.5	75.6
10	6	253.15	12,000	2.23	0.1541	69.1	72.9
11	6	253.15	12,000	2.2	0.1529	69.5	72.3
12	6	253.15	12,000	2.22	0.1574	70.9	74.5
13	6	253.15	12,000	2.22	0.1574	70.9	73.6
14	6	253.15	17,045	2.14	0.1958	91.5	88.9
15	6	261.55	12,000	1.39	0.15	107.9	102
16	8	248.15	9000	2.34	0.1806	77.2	80
17	8	248.15	15,000	2.21	0.2376	107.5	108.4
18	8	258.15	9000	1.95	0.1745	89.5	93.9
19	8	258.15	15,000	1.91	0.2355	123.3	126.6
20	9.36	253.15	12,000	2.32	0.2536	109.3	113.3

crystals grow fast and perpendicularly to the cold plate surface and forming shape is very thin and long.

Fig. 5 shows the frost images for various airflow Reynolds number at the cold plate temperature of −20 °C and at the airflow humidity of 6.0 g/kg′. As the results, airflow velocity has minor effect on frost structure and shows similar structure after 10 and 30 min. However, frost density is affected by airflow velocity as shown in Table 1 due to more intensive mass transfer.

Fig. 6(a) shows the contour plot of frost density as function of cold plate temperature and airflow humidity at the constant airflow Reynolds number of 9000 and Fig. 6(b) shows the frost images for various test conditions. Frost structure at low humidity is less porous than grass-type crystals and its thickness is smaller. At high humidity and low temperature, very porous feather-type frost structure is formed as shown in test number 23 and 19 of Fig. 7(b). Meanwhile, plate-type frost structure is formed at low airflow humidity and low cold plate temperature as shown in test number 1 in Fig. 7(b). Fig. 7(a) shows the positions of test conditions on the axes of airflow humidity and cold plate temperature in this study. It also shows the comparison with the frost map developed by Hayashi et al. [1], shown as dotted line in Fig. 7(a), and provides the images of frost structures for various test conditions investigated in this study as shown in Fig. 7(b).

Frost structures are classified into three types: plate-type crystal, grass-type crystal and feather-type crystal, have similar trends with the study of Hayashi et al. [1]. However, the investigations for colder plate temperature are supplemented in the present study to consider operating conditions of home refrigeration system.

Finally, the map for frost crystal shapes for the hydrophobic surface was proposed in Fig. 8. At the ambient conditions of high airflow humidity and low cold plate temperature as the upper area on the proposed map, frost structure consists mainly of feather-type crystals having very porous structure. The proposed map shows ambient conditions for formation of plate-type crystals, which are most favorable for operation conditions of home refrigerators: frost has high density, high conductivity and do not occupy too much space inside air passage. The central area on the proposed map is the region for the frost structure consisting of grass-type crystals. The frost density decreases with decrease of cold plate temperature in this region.

3.2. Frost map for hydrophilic surface

Test sample having the DCA of 23°, plasma coated aluminum surface, was used to develop frost map for hydrophilic surface. Test conditions are the same as the conditions for hydrophobic aluminum surface as function of airflow humidity, cold plate temperature and air Reynolds number. Test conditions and test results for frost density are tabulated in Table 2. To compare with the hydrophobic surface, test results of frost density are included in the table. The comparative analyses for those results are as follows:

1. Hydrophilic surface shows lower frost density than that of hydrophobic surface at the region of higher humidity than 8.0 g/kg′: tests number of 16, 17, 18, 19 and 20.
2. The frost density of hydrophilic surface shows lower than that of hydrophobic surface at airflow humidity of 6.0 g/kg′ and plate temperature below −15 °C: tests number of 6, 8, 9, 10, 11, 12 and 13. Maximal discrepancy of frost densities between uncoated bare aluminum surface and plasma coated aluminum surface is 9.3% at the plate temperature of −28.4 °C.

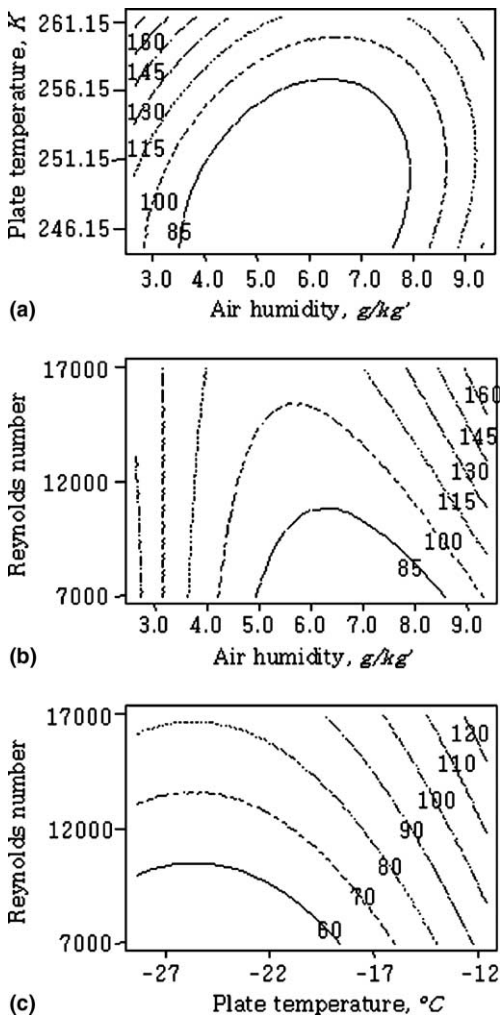

Fig. 9. Contour plots of frost density for different operating parameters on hydrophilic surface: (a) $Re = 12{,}000$, (b) $T_p = -20$ °C, and (c) $W = 6.0$ g/kg′.

3. The marked difference in frost properties were found as difference of cold plate temperature at the low airflow humidity condition of 4.0 g/kg′. The frost density of hydrophilic surface is denser about 20–30% than that of hydrophobic surface at cold plate temperature of −15 °C. But, nearly the same values were measured on both surfaces at −25 °C plate temperature.

Fig. 9 shows contour plots presenting frost density with different operating test conditions. The range of ambient conditions providing the frost formation with low density is practically the same as the range for uncoated bare aluminum surface. If cold plate temperature is within −20 to −27 °C and airflow humidity is within 4.0–8.0 g/kg′, frost density be expected below 85 kg/m^3.

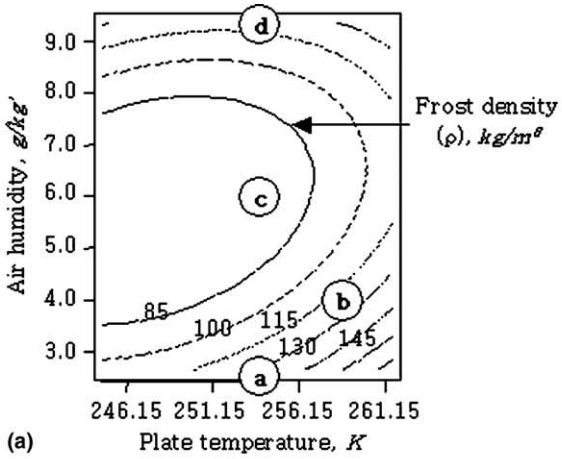

Point	Test conditions	Deposition time, min		Test No
		5	30	
a	Re = 12000 W=2.64g/kg' T_p=253.15K	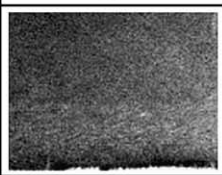	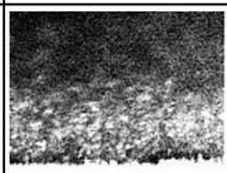	1
b	Re = 15000 W=4.0g/kg' T_p=258.15K	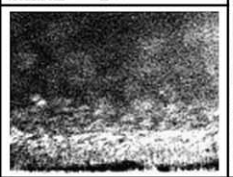	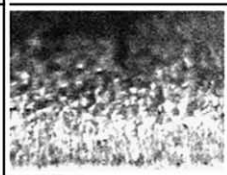	5
c	Re = 12000 W=6.0g/kg' T_p=253.15K	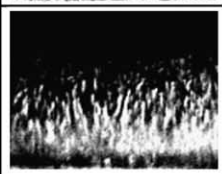	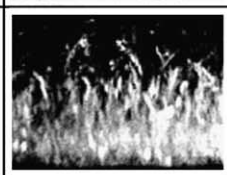	8
d	Re = 12000 W=9.36g/kg' T_p=253.15K	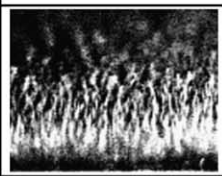		20

(b)

Fig. 10. Frost density profile for different air humidity and plate temperature and those images of frost structure: (a) contour plot and (b) frost images.

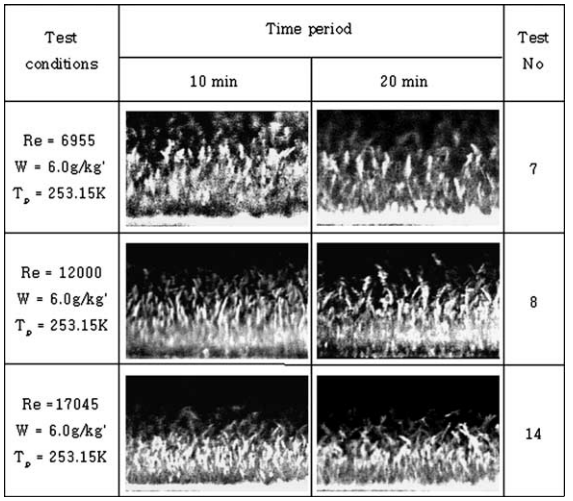

Fig. 11. Frost structures for different Reynolds number after 10 and 20 min on hydrophilic surface.

For small air Reynolds number about 7000, frost density drops even below 60 kg/m^3 as on the hydrophobic surface. Such a phenomenon may be explained by grass-type frost structure for this region as shown in image of test number 8 from Fig. 10.

Fig. 10(a) shows the contour plot for frost density as function of plate temperature and airflow humidity and frost images after 5 and 30 min. Even after 5 min frost structures differ significantly at different conditions. But, frost structures contain similarities after 5 and 30 min at same test condition. High humidity (d) provides feather-type crystals, while low humidity (a) provides plate-type crystals.

Fig. 11 shows the frost images for various air Reynolds number at airflow humidity of 6.0 g/kg′ and plate temperature of −20 °C. Air velocity has minor effect on frost structure and frost density depends on air velocity due to increase of mass transfer as the phenomenon of hydrophobic surface. However, air velocity plays important role for frost density levels comparing with that of hydrophobic surface as shown in Table 2. In addition, hydrophilic surface provides formation of less porous frost at all velocities as shown in Fig. 11 comparing the structure of hydrophobic surface as shown in Fig. 5.

Fig. 12 provides the images of frost structures on the hydrophilic surface for the test conditions in present study and classified into three main types the same as on the hydrophobic surface: feather-type, grass-type and plate-type crystal. At high humidity and low plate temperature, very porous feather-type frost structure is generated as shown in test number 20, 19 and 16 of Fig. 12. Grass-type frost structures are shown in test number 15, 8, 6 and 2 of Fig. 12. In this region, frost density is considerably decreased as the decrease of cold plate temperature and the smallest density region is similar to that of hydrophobic surface, and corresponds to the range of cold plate temperature below −25 °C and airflow humidity within 3.0–7.0 g/kg′. Meanwhile, plate-type frost structure is formed at low airflow humidity as shown in test number 4 and 1 of Fig. 12.

Fig. 13 shows the proposed frost map for hydrophilic surface comparing with that for hydrophobic surface. The regions with different frost structures are shifted

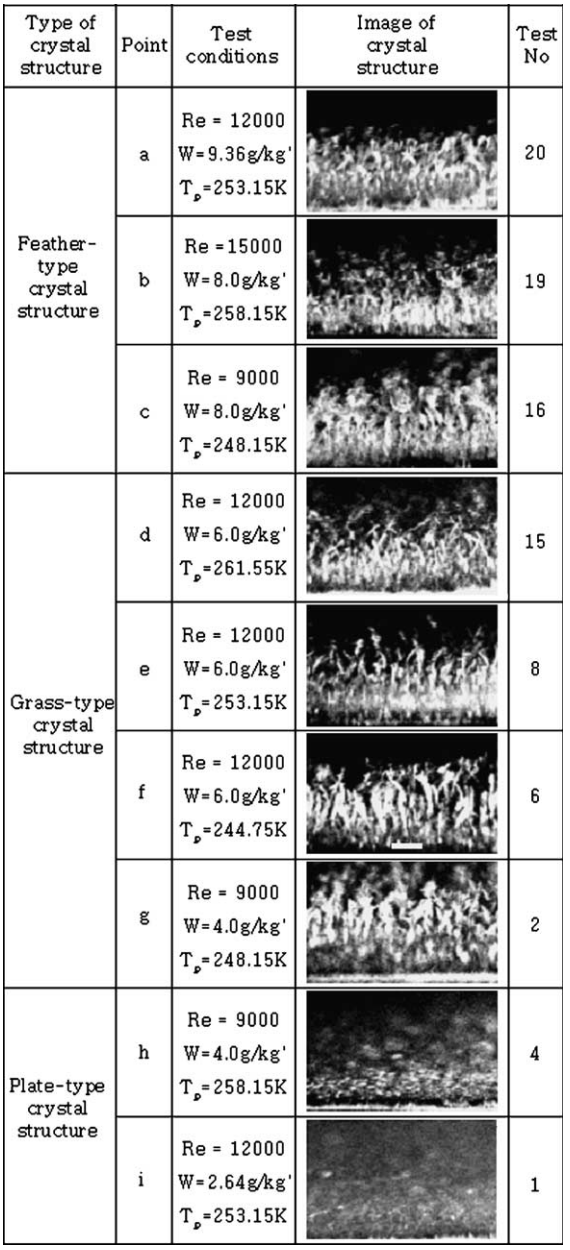

Fig. 12. Images of frost structures with the test conditions on hydrophilic surface.

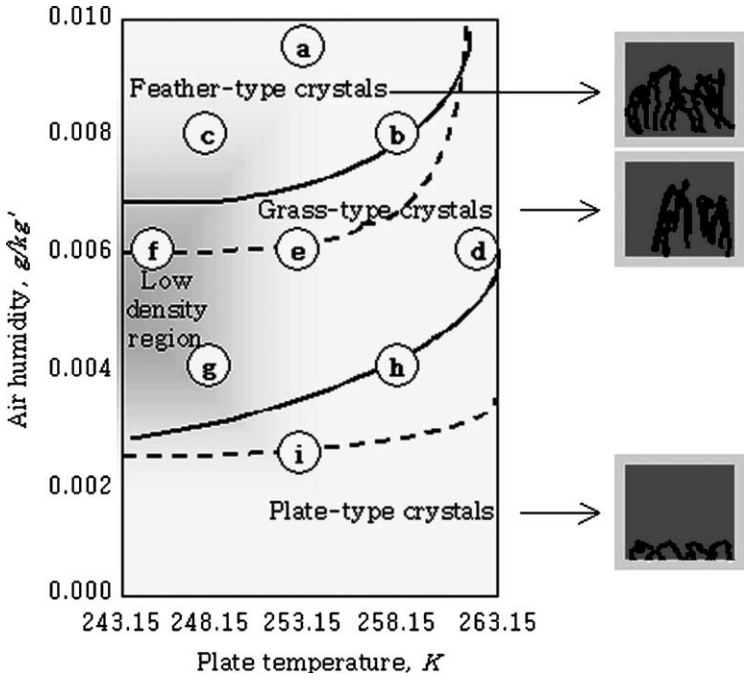

Fig. 13. Frost map for hydrophobic and hydrophilic surfaces --- hydrophobic surface (DCA = 88°), —— hydrophilic surface (DCA = 23°), ○ locations of test conditions in present study, letters inside circles corresponding to "point" shown in Fig. 12.

from dashed line for hydrophobic surface to solid line for hydrophilic surface as shown in Fig. 13. This means that denser frost is generated on hydrophilic surface than hydrophobic surface at the same test condition. That analysis can be confirmed in Table 2 with the comparison of frost density data calculated.

4. Conclusions

In the present study, frost structures are classified into three types of feather-type, grass-type and plate-type for hydrophobic and hydrophilic surfaces. Frost maps are proposed, and show ambient conditions for formation of plate-type, which are most favorable for operation conditions of home refrigerators: frost has high density and do not occupy too much space inside air passage. Frost structures are mainly depended on airflow humidity and cold plate temperature and have negligible effect for various air velocities. However, frost density is affected by air velocity due to more intensive mass transfer.

Frost structures contain similarities with the time of frost deposition on the plates at same test conditions and differ significantly at different test conditions even after 5 min. High humidity provides feather-type frost, while low humidity provides plate-type frost. In regards to frost properties, frost thickness increases as the increase of air humidity and decrease of plate temperature, but slightly affected by air velocity.

Hydrophilic surface having lower DCA has lower frost thickness and high density than hydrophobic surface having higher DCA at all air velocities. Frost structures on surface with different DCA are similar. However, regions with different frost structures are shifted and denser frost is generated on hydrophilic surface and provides 20–30% higher frost density at low air humidity condition.

References

[1] Y. Hayashi, A. Aoki, S. Adachi, K. Hori, Study of frost properties correlating with frost formation types, Trans. ASME, J. Heat Transfer 99 (5) (1977) 239–245.
[2] I. Tokura, H. Saito, K. Kishinami, Study on properties and growth rate of frost layers on cold surface, Trans. ASME, J. Heat Transfer (1983) 895–901.
[3] A.Z. Sahin, Effective thermal conductivity of frost during the crystal growth period, Int. J. Heat Mass Transfer 43 (2000) 539–555.
[4] H. Ohkubo, Effect of surface temperature on frosting phenomena, in: Proceedings of 7th International Symposium on Thermal Engineering and Sciences for Cold Regions, 2001, pp. 73–78.
[5] OSh. Hmaladze, V.P. Chepurnenko, Influence of finned surface shape on frost properties, Refrig. Tech. N2 (1986) 42–44 (Russian).

[6] K. Ogawa, N. Tanaka, M. Takeshita, Performance improvement of plate fin-and-tube heat exchangers under frosting conditions, ASHRAE Trans. 99 (1) (1993) 762–771.
[7] D.G. Nikulshina, V.L. Dol'skaya, L.S. Soigolina, V.L. Izotov, YuV. Starikh, Investigation of energy characteristics of air coolers with ceramic–organic coating, Refrig. Tech. N10 (1984) 19–21 (Russian).
[8] N. Seki, S. Fukusako, K. Matsuo, S. Uemura, Incipient phenomena of frost formation, Bull. JSME 27 (233) (1984) 2476–2482.
[9] J.L. Hoke, J.G. Georgiadis, A.M. Jacobi, The interaction between the substrate and frost through condensate distribution, Technical Report, University of Illinois, Urbana Champaign, 2000, pp. 1–135.
[10] I.S. Ryu, Y.B. Lee, S.T. Ro, The effect of environmental variables on frost formation on a horizontal cylinder, Proc. SERAK (2000) 104–108.
[11] J. Shin, A. Tikhonov, C. Kim, Experimental study on frost structure on surfaces with different hydrophilicity: density and thermal conductivity, ASME J. Heat Transfer 125 (2003) 84–94.
[12] G. Kim, H. Lee, L. Ralph, Plasma hydrophilic surface treatment for dehumidifying heat exchangers, Exp. Thermal Fluid Sci. 27 (2002) 1–10.
[13] J.M. Shin, N.G. Lee, S.J. Han, S.C. Ha, The effect of water contact angles of the fin surface of the fin-and-tube heat exchangers on the water hold-up, J. Air-Cond. Refrig. 13 (6) (2001) 490–496.
[14] ASHRAE Standards, Standards method for laboratory airflow measurements, ANSI/ASHRAE 41.2-1987 (RA 92), 1992, p. 32.
[15] K. Lee, W. Kim, T. Lee, A one-dimensional model for frost formation on a cold plate surface, Int. J. Heat Mass Transfer 40 (18) (1997) 4359–4365.
[16] Y. Mao, R.W. Besant, K.S. Rezkallah, Measurement and correlations of frost properties with airflow over a flat plate, ASHRAE Trans. 98 (1992) 65–78.
[17] R. Ostin, S. Anderson, Frost growth parameters in a forced air stream, Int. J. Heat Mass Transfer 34 (4/5) (1991) 1009–1017.